Geological Quarterly, 2023, 67: 6
DOI: http://dx.doi.org/10.7306/gq.1676

Geochemical characteristics of spherules from the Pivdenna kimberlite pipe, East Azov region (Ukraine): implications for their sources and origin

Ivan YATSENKO[1,] *, Andriy POBEREZHSKYY[1], Oksana STUPKA[1] and Serhii BEKESHA[2]

[1] Institute of Geology and Geochemistry of Combustible Minerals of National Academy of Science of Ukraine, Naukova 3a, 79060 Lviv, Ukraine; ORCID: 0000-0002-7972-1702 [I.Y.]; 0000-0002-4622-0725 [A.P.]; 0000-0001-5871-0249 [O.S.]

[2] Ivan Franko National University of Lviv, Hrushevskoho 4., 79005 Lviv, Ukraine; ORCID: 0000-0002-3275-8276

Yatsenko, I., Poberezhskyy, A., Stupka, O., Bekesha, S., 2023. Geochemical characteristics of spherules from the Pivdenna kimberlite pipe, East Azov region (Ukraine): implications for their sources and origin. Geological Quarterly, 2023, 67: 6, doi: 10.7306/gq.1676

The composition of spherules and particles of native metals from the Pivdenna kimberlite pipe, Ukraine, was studied using the SEM/EDS method. Three varieties of spherules have been distinguished: titanium-manganese-iron-silicate (TMIS) spherules, Ca-rich silicate spherules, and magnetite-wustite-iron (MW-I) spherules. TMIS spherules are composed of homogeneous glass, some having a native iron core. Large TMIS spherules may contain a crystalline phase with needle-like armalcolite. Ca-rich silicate spherules can be subdivided into two subtypes: calcium-silicate (CS) spherules where SiO_2 and CaO are the dominant constituents, and calcium-iron-silicate (CIS) spherules with significant FeO content. CS spherules may contain a core consisting of native phases (Fe, Fe-Si, and Mn-Si-Fe). Native metal particles are represented by native Cu and native Zn. The spherule varieties from the Pivdenna pipe are similar to those from other kimberlite pipes in the world. We infer that the formation of spherules occurred in gas-melt streams, separately from the kimberlites, and propose a model for the formation of the most common variety of spherules (TMIS and MW-I varieties) in the region of the core-mantle boundary (CMB). First, a melt of the Fe-Ti-Mn-Si-O system was formed in ultra-low-velocity zones (ULVZ) as a result of thermochemical reactions (reduction) between the molten core and solid oxide-silicate rocks. The melt then migrates to shallower levels, where a decrease in temperature initiates oxidation with the formation of SiO_2-TiO_2-FeO-MnO-Fe^0 melt, i.e. parent melt of TMIS and MW-I spherules. We interpret the formation of native metals in kimberlites as a result of the decomposition of nitrides, which came from the Earth's core via intratelluric flows.

Key words: spherules, kimberlites, native metals, core-mantle boundary, ULVZ.

INTRODUCTION

The late Latin word “spherule” is a diminutive of the Latin “sphaera”. In the scientific literature, it is used to describe small spherical objects. In geology, this term has a genetic connotation and is used to define spherical droplets formed from a melt or as condensate from a vaporized substance (Hefferan and O’Brien, 2010). Spherules have been found in various geological formations around the world: in oceanic sediments of the Pacific (Robin et al., 1993), Atlantic and Indian oceans (Glass et al., 1985); on continents in the K-T boundary layers (Grachev et al., 2008) and in many other sedimentary deposits (Uzonyi et al., 1998; Berczi et al., 1999; Firestone et al., 2007; Yatsenko et al., 2013a). Spherules have also been found in Antarctica ice (Taylor et al., 2000), Greenland ice (El Coresy, 1968), the ice cap of Novaya Zemlya (Badjukov and Jouko, 2003), and in deposits associated with impact ring structures (Fredriksson et al., 1973; Hodge, 1973; Graup, 1981). Spherules have also been found in lunar soil (Brown et al., 1970; Culler et al., 1997). Broadly, the known spherule suite can be divided into two main types. The first, the so-called I-type, is made of iron oxides and may incorporate a core of native iron (El Coresy, 1968; Taylor et al., 2000). Glassy spherules are the second type; in many cases, glass spherules may contain a crystalline phase (olivine, pyroxene, and iron oxides) within the glass matrix. The two main hypotheses on spherule origin are widely reported. Some authors consider them as a result of the ablation of extra-terrestrial particles during atmospheric entry, while others interpret spherules as the product of the condensation of evaporated matter during impact events. In most cases, it is difficult to accurately recognize the true nature of such spherules. In many cases, the geochemical characteristics of spherules do not confirm their extra-terrestrial nature, and many finds of spherules are difficult to correlate with distinctive impact events. Moreover, there are many occurrences where spherules have been interpreted as the unequivocal products of magmatic processes (O’Keefe, 1986; Rychagov et al., 1997; Peskov, 2000; Novgorodova et al., 2003; Morgan et al., 2004; Medvedev et al., 2006; Lukin, 2006, 2013; Chaikovsky and Korotchenkova, 2012; Griffin et al., 2018).

---

* Corresponding author, e-mail: yatsenko.ivan1000@gmail.com

Received: September 15, 2022; accepted: January 12, 2023; first published online: Ferbruary 27, 2023

This paper presents the results of the study of spherules collected from kimberlites of the Pivdenna pipe in East Azov region of the Ukraine. A distinctive feature of this spherule suite is that it includes a significant number of transparent Ca-rich silicate spherules (Vaganov et al., 1985; Bratus et al., 1987). We have not encountered this spherule type in previously studied kimberlites of the Ukrainian Shield. We summarized the published information on them and drawn together the results of our previous studies of spherules from kimberlite structures to describe the general characteristics of the kimberlite spherule varieties. We consider questions related to the physical mechanism of spherule formation and general questions concerning the relationship between kimberlites and highly reduced mineral particles such as spherules. We propose a modified model for the formation of the commonest spherule types such as the TMIS and MW-I varieties. We also propose a possible mechanism for the formation of Cu, Zn, Sn, and Pb metallic particles, which commonly occur in kimberlitic rocks.

PREVIOUS WORK

In this article, we focus on the study of distinctive spherule types encountered in kimberlite rocks. Originally, these spherules were discovered in the kimberlites of the Udachna pipe, Yakutian diamondiferous province (Tatarintsev et al., 1983), where three spherule types were identified. The first type comprises magnetic spherules composed of magnetite and wustite with or without a metallic iron core (MW-I spherules). The second type consists of opaque spherules and scoriaceous particles of silicate glass with a significant amount of TiO_2, MnO and FeO (TMIS spherules). Some of these spherules contain an iron core. Spherule glass may contain Mn-ilmenite, armalcolite, rutile, and ulvöspinel microlites. The third type comprises greenish transparent glass spherules, some with inclusions of native iron. Spherules of this last type can have different shapes: spherical, elliptical, dumbbell-shaped, and teardrop-shaped. Marshintsev (1990) carried out a more detailed study of spherules from the kimberlites of the Yakutian province (Mir, Aikhal, and Udachna pipes), recognizing that the third spherule type is made of glass, where Ca is a dominant constituent (~40%) and a significant amount of Al (10–12%) is present. Yatsenko (2016) coined the term calcium-aluminium-silicate spherules (CAS) for this spherule type. Vaganov et al. (1985) described spherules from the East Azov kimberlite pipes and the Udachna pipe and spherules from explosive structures that are interpreted to be impact structures (Kara, Belylivka, Illintsi and Bovtyshka structures). In all cases, the same three types of spherule noted above were distinguished (Tatarintsev et al., 1983; Marshintsev, 1990). Detailed geochemical studies of spherules from diamond-bearing tuffisites of the Western Urals were described by Chaikovsky and Korotchenkova (2012). The authors divided the above types of spherule into many subgroups, and estimated the melting temperature of various types of glass spherule in the range from 1200 to 2100°C. Findings of MW-I, TMIS and CAS spherule varieties collected from the kimberlites of the Catoca and Txiuzo pipes (Angola) were reported by Zinchenko et al. (2012).

In our previous work, we described spherules found in kimberlite-like structures of the Ukrainian Shield (Mriya and Zelenyi Gay pipes, Shchors dyke, and Gruz'ka-Pivnichna explosive structure), kimberlites of the Arkhangelsk (Karpinska pipe) and Yakutian diamondiferous provinces (Yatsenko et al., 2012a, 2020; Yatsenko, 2016). The rocks of these structures were found to contain various proportions of MW-I and TMIS spherules. The studies showed that in most cases, in association with spherules, other varieties of highly reduced mineral particle occur, including native metals (Cu, Zn, Sn, Pb) and their intermetallic alloys; oxygen-free minerals (WC, SiC); and Ti corundum with inclusions of Fe, Fe-Si, Fe-Ti-Si, TiN, and TiC phases (Yatsenko, 2016; Yatsenko et al., 2020). We have grouped spherules and other highly reduced mineral particles into one class of matter which termed the high-reduced mantle mineral association (HRMMA). We have shown that the required conditions for the formation of HRMMA are very difficult to reconcile with kimberlite formation processes. In the concept proposed (Yatsenko, 2016; Yatsenko et al., 2020), the formation of HRMMA is associated with thermochemical processes in the lowermost mantle (layer D'').

GEOLOGICAL OVERVIEW

The Pivdenna kimberlite pipe together with other Devonian pipes such as Nadiya, Novolaspinska, Petrivska and also with other kimberlite bodies (dykes) form the Petrivsk-Kumachevo kimberlite field (Geiko et al., 2006). This kimberlite field is located in the northern part of the East Azov subblock of the Ukrainian Shield, in the zone of its junction with the Donbas (Fig. 1A, B). The pipe has an irregular "amoeboid" surface plain form, 150 to 300 m across, of surface outcrop ~2.2 ha in area (Fig. 1C). The kimberlite body is overlain by Quaternary deposits 8-10 m thick (Fig. 1D). Emplaced into syenites of the Khlibodarivka Unit of the Paleoproterozoic are massive kimberlites of Group 2 variety (micaceous kimberlites enriched in phlogopite) and kimberlite breccias (Sheremet et al., 2014). (Group 1 kimberlites are typified by abundant olivine and groundmass perovskite, spinel and monticellite or calcite: Sparks et al., 2006). The kimberlite breccia consists of kimberlitic material (60–70%) and xenogenic material, which is made of accidental lithic clasts of host-country rock including different varieties of syenite, and Devonian limestones and sandstones. Mantle xenoliths are represented by pyrope and ilmenite peridotites. The upper part of the pipe to a depth of 30-40 m is made up of weathered kimberlites (Fig. 1D). In the central part of the pipe, there are "floating reefs" of granitoids up to several tens of metres across.

SAMPLING AND METHODS

Spherules were extracted in the concentrate obtained from the core of boreholes SV219/24 (10–16 m depth) and SV730 (15–25 m depth). The first stage of processing included multistage crushing to the 0.5–1 mm fraction. The weight of the crushed samples was ~15 kg. Then the samples were washed with water on a concentration table to remove sludge and light fraction minerals. Processing was carried out until a "grey concentrate" was obtained (Sheremet et al., 2014). Spherule and other spherule-like particles were hand-picked from the heavy mineral separate using a binocular microscope. The preparation of samples for microanalytic investigation included several stages. At first spherule samples were mounted in epoxy. After solidification, slides with samples emplaced in epoxy were ground and polished to show the maximum cross-sectional area of each grain. Finally, a polished block 17 mm across with mounted polished grain samples was coated with a carbon film. Spherule samples were observed using a REMMA-102-02 scanning electron microscope (SEM); images were taken using

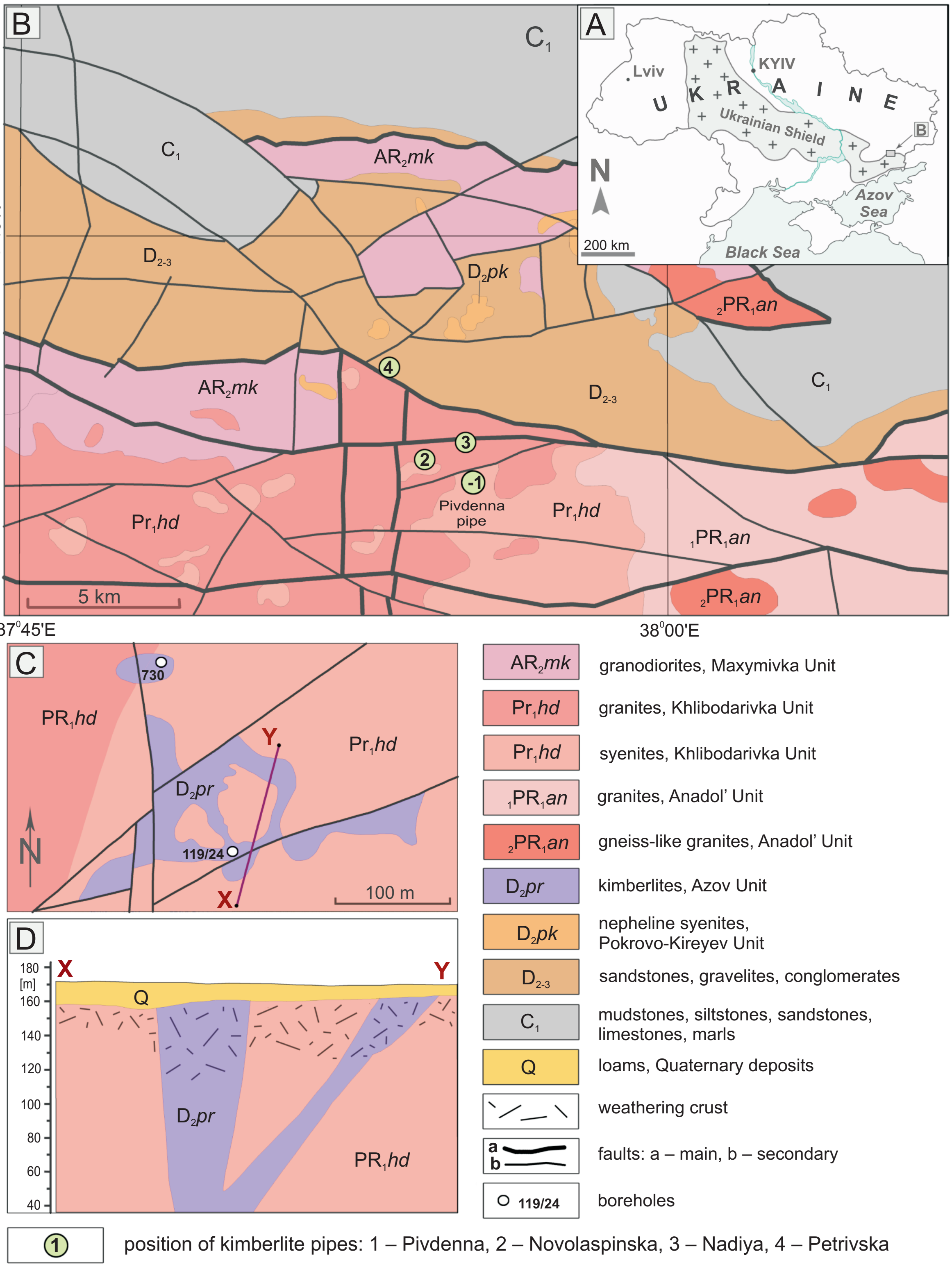

Fig. 1A – position of the Ukrainian shield (modified after Gursky, 2008), with the location of the study area; B – position of Devonian kimberlite pipes on the geological map; C, D – surface outline of the Pivdenna pipe and its vertical section along the X–Y line (modified after Sheremet et al., 2014)

backscattered electron (BSE) mode. Chemical compositions were obtained by an EDAR energy-dispersive spectrometer (EDS) attached to the SEM. The samples were analysed with an accelerating voltage of 20 kV and a sample current of 1 nA with a point beam 0.1 μm in diameter. Calibration by Cu; W cathode was used. The instrument was calibrated according to mineralogy set standards *NERMA.GEO1.25.10.74GT. Magallanes 3.2* software has been used.

RESULTS

Based on the chemical composition, the suite of spherules collected in the Pivdenna pipe can be subdivided into three main types (Fig. 2) including Ca-rich silicate spherules (Fig. 3), TMIS spherules (Fig. 4), and MW-I spherules (Fig. 5A–H). Ca-rich silicate spherules were subdivided into two subtypes, which differ in iron content (Fig. 2). All spherule types from the Pivdenna pipe have been previously described from various kimberlite-lamproite explosive structures as noted in “Previous Work” above. In most cases, the spherules contain inclusions of native iron, which indicate that they formed under extremely reducing conditions. This allowed us to consider spherules as a component of a HRMMA. A representative assemblage of HRMMA particles was recognized in samples from borehole SV730. The assemblage includes Ca-rich silicate spherules, TMIS spherules, MW-I spherules, and native metal particles including Cu and Zn (Fig. 5A–H). Ca-rich silicate spherules are the dominant component, the remaining components being subordinate. The total concentration of the HRMMA in the sample from SV730 is ~4%. In the concentrate from the borehole SV219/24, a small amount of TMIS spherules was collected, its content not exceeding 0.1%. Some samples of TMIS and MW-I particles can be as large as 4 mm across; these lose their sphericity and appear as slag-like particles termed here scoriaceous particles.

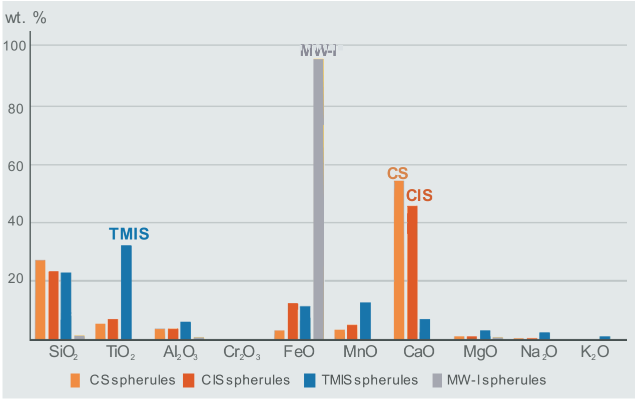

Fig. 2. Average chemical composition of spherule types identified from the Pivdenna pipe

Ca-RICH SILICATE SPHERULES

Micrographs of typical varieties of Ca-rich silicate spherules are shown in Figure 3. The size of spherules varies from 0.3 to 1 mm. Spherules consist of transparent, translucent or opaque glass of various colours. The variety of colour shades is illustrated in Figure 3. In most cases, the spherules are spherical, but ellipsoidal varieties (Fig. 3E) and various combinations of double aggregates occur (Fig. 3F, G). Some samples may have a considerable content of gas bubbles (Fig. 3G, H). The chemical composition of Ca-rich spherule glass is shown in Table 1. Ca-rich silicate spherules can be subdivided into two subtypes. The main type comprises calcium silicate (CS) spherules. The dominating components of glass are Ca (30–60 wt.%) and Si (20–37 wt.%). Notable amounts of Ti, Al, Mn, and Fe are present, the total of these elements not exceeding 15% (Table 1). These varieties usually are made of transparent glass in mostly pale shades. Some spherules contain a core of native Fe or intermetallic alloys of the Fe-Si and Mn-Si-Fe systems (Table 2). Another subtype of Ca-rich spherule comprises spherules with a significant iron content ranging from 10% up to 20% in some cases (Table 1). A characteristic feature of this variety is its black colour. We term these calcium-iron-silicate (CIS) spherules.

TMIS SPHERULES AND SCORIACEOUS PARTICLES

Micrographs of typical TMIS (titanium-manganese-iron-silicate) spherules are shown in Figure 4. In most cases, they have a regular spherical shape (Fig. 4A–E), rarely ellipsoidal (Fig. 4A–E); the spherule size ranges from 0.1 to 0.5 mm. Spherules exceeding 1 mm in size are rare, these mostly being irregular and resembling scoriaceous particles (Fig. 4G, I). The colour varies from deep black to dark brown. The surface can be smooth and shiny, in some cases rough, and they may contain gas bubbles. Small spherules (up to 0.5 mm) consist entirely of homogeneous glass. The glass may contain spherical micro-inclusions of native iron (Fig. 4H and Table 2) 1–10 m in size. The composition of TMIS glass spherules is shown in Table 1. The dominant components are Ti, Si, Mn, and Fe. In larger spherules and scoriaceous particles, a crystalline phase commonly occurs, represented by needle-like crystals of armalcolite. In this case, the residual glass of the matrix is relatively enriched in SiO_2 (24–33%), Al_2O_3 (7–8%), and CaO (9–15%).

MW-I SPHERULES AND SCORIACEOUS PARTICLES

MW-I spherules are in most cases spherical, rarely double-shaped; spherule size is in the 0.1–0.5 mm range (Fig. 5A–E). MW-I scoriaceous particles are flattened, larger (1–1.5 mm), and contain significant amounts of gas bubbles (Fig. 5F–H). MW-I particles are dark grey or black and have a metallic lustre. Some spherules consist entirely of iron oxides, others contain a core of native iron (Fig. 4H and Table 2). Iron oxides (magnetite and wustite in various proportions) contain minor impurities (up to 2%) SiO_2, TiO_2, Cr_2O_3, Al_2O_3, MnO and CaO. The iron cores of spherules also contain an admixture of these metals (Table 2).

NATIVE Cu, Zn

Native copper occurs as elongated brown grains, up to 2 mm long (Fig. 5I). Native zinc occurs as elongated and lamellar grains of bluish-grey colour; grain size ranges from 0.5 to 1.5 mm. Most Zn grains are enveloped by zinc carbonate or zinc oxide (Fig. 5J, K).

INTERPRETATION OF RESULTS

Ca-RICH SILICATE SPHERULES (CS AND CIS VARIETIES)

Some varieties of Ca-rich silicate spherules, from their chemical composition, should be interpreted as transitional varieties between CS and CIS varieties. CS spherules also contain iron, though not in the glass composition; they contain iron

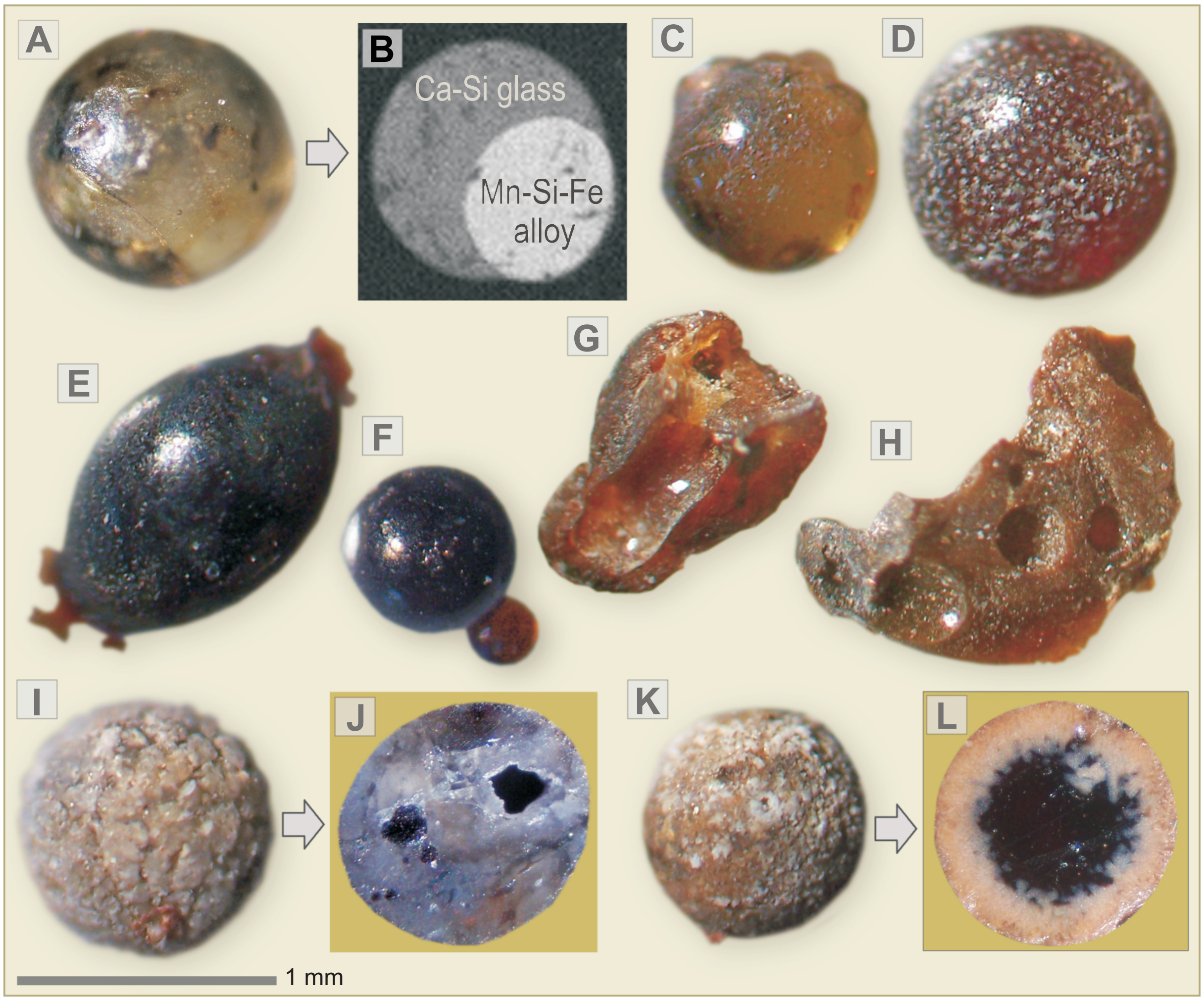

Fig. 3. Micrographs of CS spherule varieties and some features of their internal structure

A – greenish spherule; **B** – the same spherule, cross-section, BSE-image; **C** – greenish-yellow spherule; **D** – red spherule; **E** – spindle-shaped spherule; **F** – double spherule; **G, H** – fragments of red-brown spherules; **I** – opaque spherule; **J** – the same spherule, cross-section, reflected light; **K** – brown opaque spherule; **L** – the same spherule, cross-section, reflected light

forming spherical inclusions of native iron. Thus, we can interpret the CS spherule as a more reduced version of the CIS variety of glass.

Spherules very similar to the distinguished CS varieties were described by Chaikovsky and Korotchenkova (2012), collected from diamond-bearing pyroclastic rocks of the Western Urals. These authors also identified another variety of Ca-rich silicate spherule with a significant content of Al_2O_3 (CAS spherules). Similar CAS spherules were described by Marshintsev (1990) in the kimberlites of Yakutia. We have identified this variety of Ca-rich silicate spherule in Paleogene volcaniclastic deposits of the Western Slope of the Ukrainian Shield (Putryntsi Site) together with other HRMMA components (Yatsenko, 2016): in Cretaceous strata of the SW margin of the East European Platform and the Neogene deposits of the Carpathian region (Uzonyi et al., 1998; Berczi et al., 1999; Yatsenko, 2013a).

Using the phase diagram of Gentile and Foster (1963), the melting temperatures of glass CS spherules from the Pivdenna pipe were estimated in the range of 2000–2100°C (Fig. 6). This result is consistent with the data obtained by Chaikovsky and Korotchenkova (2012).

TMIS PARTICLES (SPHERULES AND SCORIACEOUS PARTICLES)

TMIS particles from the Pivdenna pipe are very similar to those discovered in the kimberlite-like structures of the Ukrainian shield (Mriya pipe, Zelenyi Gay pipe, Gruz'ka-Pivnichna explosive structure, Shchors kimberlite dyke), Arkhangelsk and Yakutian diamondiferous provinces (Yatsenko et al., 2012a, 2020; Yatsenko, 2016). They are also very similar to TMIS particles from the kimberlites of the Mir and Udachna pipes, Yakutia (Tatarintsev et al., 1983; Marshintsev, 1990); the Catoca and Thiuzo pipes, Angola (Zinchenko et al., 2012); intrusive pyroclastic rocks of the Western Urals (Chaikovsky and Korotchenkova, 2012); volcanoclastic rocks of the Kamchatka region (Rychagov et al., 1997; Sandimirova et al., 2003); and the Belylivka impact structure (Tsymbal et al., 1999). Taken together, the available data indicate that TMIS are the commonest component of the HRMMA from kimberlite-like rock and are predominantly composed of TiO_2, SiO_2, FeO and MnO with subsidiary constituents of CaO, Al_2O_3 and MgO (Table 1). Some spherules have CaO content as high as 10%, however,

Table 1

Major element composition of spherule glasses from the Pivdenna pipe [in wt.%]

Spherule types		Lab. no	SiO_2	TiO_2	Al_2O_3	Cr_2O_3	FeO	MnO	CaO	MgO	Na_2O	K_2O	Total
Ca-rich silicate spherules	CS spherules	1YU-36	37.57	1.58	4.11	0.24	1.48	2.89	50.90	0.94	0.23	0.06	100.00
		1YU-37b	23.12	5.18	3.79	0.27	4.35	4.63	56.04	1.24	1.37	0.00	100.00
		1YU-38	29.65	2.23	3.42	–	3.66	1.78	58.15	0.91	0.20	0.00	100.00
		1YU-46	25.20	5.24	4.04	0.08	5.34	2.00	56.87	0.89	0.08	0.27	100.00
		1YU-48	27.10	5.53	3.47	0.04	3.77	3.55	54.95	1.10	0.49	0.00	100.00
		1YU-39	26.92	5.99	3.54	–	2.07	3.73	55.50	1.65	0.60	0.00	100.00
		1YU-40a	23.75	5.84	6.00	0.20	0.51	5.13	56.13	1.69	0.58	0.17	100.00
		1YU-40b	16.83	20.60	5.14	0.65	1.09	4.72	48.82	1.42	0.32	0.39	100.00
		1YU-41a	37.00	0.75	3.59	0.42	1.21	0.30	54.18	1.48	0.97	0.09	100.00
		1YU-42	25.85	2.71	2.48	–	2.21	3.98	59.95	1.97	0.85	0.00	100.00
		1YU-43	29.83	5.71	5.00	0.07	1.96	2.23	51.46	1.86	1.51	0.36	100.00
		1YU-44	28.51	0.73	3.41	0.62	1.74	1.44	61.91	1.03	0.28	0.34	100.00
		1YU-45	24.73	6.45	4.28	0.41	1.56	4.37	56.91	1.16	0.07	0.06	100.00
		1YU-49	25.68	8.70	4.15	0.18	5.23	2.48	51.97	1.08	0.24	0.29	100.00
		1YU-50	26.32	4.97	3.61	0.16	6.42	6.14	48.86	1.59	1.57	0.38	100.00
		1YU-51	25.60	6.34	4.66	0.24	5.98	2.48	53.56	0.95	0.10	0.09	100.00
		1YU-52	24.48	7.15	3.85	0.38	2.93	2.56	56.58	1.04	0.86	0.17	100.00
		1YU-54	29.20	4.48	3.46	0.29	6.16	8.45	43.23	1.54	3.13	0.06	100.00
		1YU-12	23.45	6.83	4.15	0.31	11.17	5.05	47.54	1.26	0.22	0.00	100.00
		1YU-13	23.42	5.44	4.66	0.75	11.53	1.84	50.82	1.52	–	0.02	100.00
		1YU-14	22.87	6.85	4.14	0.44	7.91	7.64	47.41	1.38	1.30	0.06	100.00
		1YU-15	21.49	3.97	4.25	0.46	14.13	4.67	48.32	1.55	1.08	0.08	100.00
		1YU-16	20.70	12.83	4.30	0.99	18.66	4.38	37.33	0.66	–	0.14	100.00
		1YU-17	24.07	4.48	4.20	0.45	9.95	6.53	47.67	1.15	1.49	0.00	100.00
		1YU-18	21.62	7.13	3.62	0.41	9.68	2.33	54.15	0.98	–	0.07	100.00
		1YU-19	23.90	4.40	3.76	0.51	9.07	6.74	49.22	1.20	1.17	0.02	100.00
		1YU-20	20.83	5.58	4.06	0.42	16.38	2.84	49.22	0.59	–	0.08	100.00
		1YU-21	21.95	7.52	3.60	0.66	19.36	6.09	39.38	1.17	0.25	0.02	100.00
		1YU-37a	23.05	8.94	4.76	0.52	8.09	2.30	50.07	1.43	0.81	0.04	100.00
		1YU-47	25.22	7.24	3.11	0.02	10.04	3.16	49.24	1.44	0.36	0.17	100.00
		1YU-53	28.44	12.59	4.34	0.14	8.17	11.01	30.01	3.50	1.13	0.67	100.00
		1YU-62	24.17	6.96	2.92	0.19	20.17	6.39	37.54	1.28	0.29	0.10	100.00
TMIS spherules		1YU-1	23.97	26.40	8.34	0.43	13.06	13.08	8.89	2.74	2.09	1.01	100.00
		1YU-3	29.73	22.03	6.86	0.08	7.48	11.61	15.41	2.71	3.06	1.03	100.00
		1YU-26	20.09	34.34	5.64	0.28	15.11	13.53	4.62	3.04	2.36	0.98	100.00
		1YU-27	20.13	36.35	5.14	0.55	13.38	12.33	5.51	3.16	2.55	0.90	100.00
		1YU-28	19.96	34.75	5.37	0.30	13.33	13.87	5.29	3.25	2.85	1.03	100.00
		1YU-29	32.66	17.62	6.93	0.29	6.57	17.61	10.31	2.58	3.93	1.49	100.00
		1YU-30	21.41	39.17	5.75	–	6.82	13.31	5.46	3.55	3.11	1.43	100.00
		1YU-31	21.05	34.32	5.60	0.11	15.90	11.29	5.10	3.40	2.50	0.72	100.00
		ZG-8	21.86	33.90	5.93	0.35	13.94	10.12	5.90	4.21	2.32	1.47	100.00
		ZG-9	18.85	42.33	6.41	0.27	8.35	10.35	6.54	3.51	1.91	1.47	100.00

there are no examples of spherules that could represent transitional varieties between Ca-rich and TMIS spherules.

TMIS scoriaceous particles contain a crystalline phase represented by needle-like and skeletal crystals of Mn-ilmenite, armalcolite, ulvöspinel, and rutile. The cooling of the spherules occurred instantly with the formation of homogeneous glass. Larger scoriaceous particles cooled slightly more slowly, which enabled the formation of a crystalline phase. The study of the major components of various TMIS spherules showed that the kind of mineral of the crystalline phase depended on the initial ratio of the mineral-forming components TiO_2, FeO, and MnO in the initial melt (Yatsenko et al., 2012a). Ulvöspinel is formed in rare cases when the FeO content prevails over TiO_2 and MnO. In most cases, TiO_2 and MnO are dominant and thus we observe the formation of Mn-ilmenite and armalcolite.

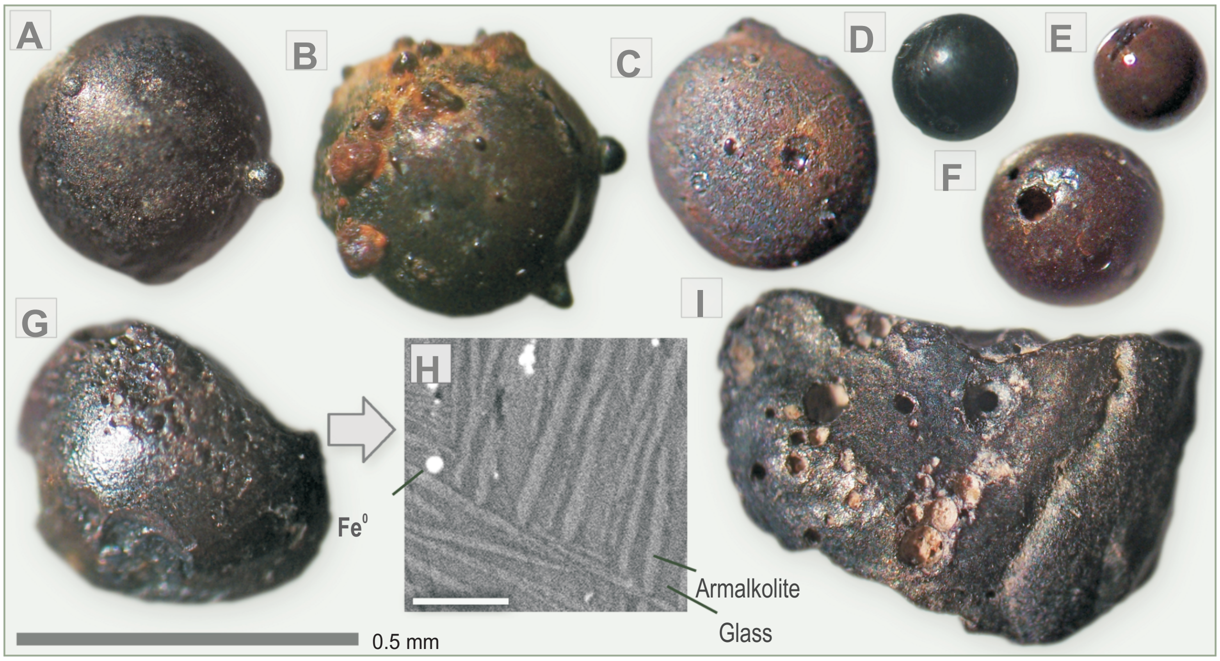

Fig. 4. Micrographs of TMIS spherules

A–G – micrographs of spherules showing their characteristic forms and surface textures; **H** – internal texture of a spherule (G) which is made of needle-like crystals set in a glassy matrix, BSE image**;** **I** – scoriaceous TMIS particle

Table 2

The composition of metallic inclusions in spherules [in wt.%]

Spherule type with metallic inclusions	Lab. no	Metals, alloy	Si	Ti	Al	Cr	Fe	Mn	Ca	Mg	Na	K	Total
CS	1YU-36	Mn-Si-Fe	23.45	3.11	0.60	0.26	60.42	11.57	–	0.57	–	0.01	100.00
CS	1YU-37	Fe	0.64	0.11	0.69	0.24	97.01	0.06	0.40	0.47	0.34	0.05	100.00
CS	1YU-41A	Si-Fe	23.09	2.63	0.84	0.48	66.13	5.40	–	0.72	0.70	–	100.00
TMIS	1YU-1	Fe	1.57	4.72	1.39	0.17	88.91	0.73	1.17	0.96	0.29	0.08	100.00
MW-I	1YU-55	Fe	0.61	0.07	0.73	0.21	98.11	–	–	0.27	–	–	100.00
MW-I	1YU-56	Fe	0.51	0.22	0.65	–	97.99	–	0.04	0.56	–	0.02	100.00
MW-I	1YU-57	Fe	0.49	0.08	0.63	0.20	97.66	–	0.04	0.71	0.19	–	100.00
MW-I	1YU-35	Fe	0.47	0.03	0.58	0.16	98.56	–	–	0.20	–	–	100.00
Individual metal particles	ZG-15	Fe	–	0.10	–	0.46	99.27	0.17	–	–	–	–	100.00

MW-I SPHERULES AND SCORIACEOUS PARTICLES

MW-I together with TMIS spherules are the common spherule types that have been found in the Pivdenna pipe and all previously studied kimberlite-like structures in Ukraine. Moreover, the MW-I and TMIS varieties invariably occur together. We assume that these two spherule types, formed by explosive processes, are genetically close to each other, i.e., they come from the same metal-silicate melt source.

The MW-I type is the most common of all known spherule varieties. An analysis of published data has shown that MW-I spherules represent the commonest spherule type encountered worldwide in a wide variety of volcanic and sedimentary deposits (El Coresy, 1968; Bratus et al., 1987; Berczi et al., 1999; Taylor et al., 2000; Badjukov and Jouko, 2003; Medvedev et al., 2006; Grachev et al., 2008; Lukin, 2013; Griffin et al., 2018). As some industrial processes (e.g., electric welding) show, the formation of MW-I spherules is a simple process caused by the oxidation of red-hot iron fragments. Thus, it is clear that MW-I spherules, which are quite commonly found in various deposits, can have a cosmogenic, impact, technogenic or endogenous origin, i.e. to be a product of different high-temperature processes.

NATIVE Cu, Zn

Native Au and Cu particles from borehole SV219/24 (Pivdenna pipe) were reported by Tischenko (2004). Native Cu and Zn were found by us in borehole SV730. Tischenko's data and our new findings corroborate our previous observations, which suggest that native metal particles are a constant component of the HRMMA from kimberlite-like rocks. Particles

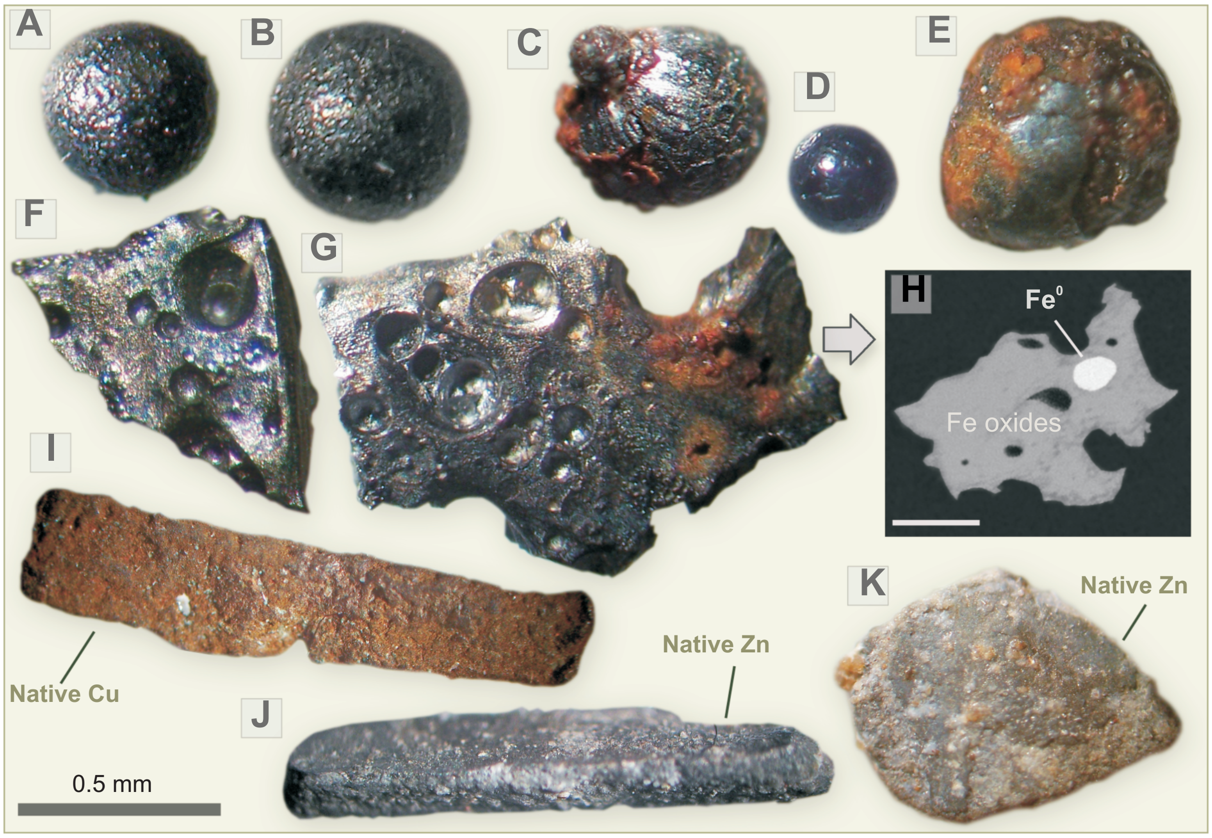

Fig. 5. Micrographs of MW-I spherules and native metal particles

A–E – typical MW-I spherules; **F, G** – MW-I scoriaceous particles, numerous gas bubbles are visible on the surface; **H** – cross-section through the previous sample, BSE image; **I** – an elongate particle of native copper; **J** – an elongate particle of native zinc; **K** – lamella of native zinc

of native metals and intermetallic alloys have been identified in all previously studied explosive structures (Yatsenko, 2016, 2020) including the Mriya lamproite pipe (Fe, Pb, Sn, Sn-Pb, Sb-Pb, Zn-Cu, Au), the Zelenyi Gay pipe (Fe, Cu-Zn), the Gruz'ka-Pivnichna kimberlite structure (Cu-Zn), and the Karpinska kimberlite pipe (Cu). The common presence of native metal mineralization in kimberlites was convincingly demonstrated by Makeyev and Kriulina (2012), who discovered films of native metals on the surface of diamonds from the Yakutsk and Arkhangelsk diamondiferous provinces. The films consist of 15 chemical elements that occur in the form of native metals and their intermetallic alloys. Many single particles of native metals take a spherical or plastic form, indicating that the mechanism of formation of spherules and metal particles was similar (Yatsenko, 2020). In essence, particles of native metals can be referred to as spherule-like particles formed in a fluid environment.

Ti-BEARING CORUNDUM

A specific variety of Ti-bearing corundum (Ti_2O_3 – 0.5–2%) was first discovered in kimberlites of the Eastern Azov region (Tatarintsev et al., 1987), with several subsequent finds of this mineral in mantle rocks elsewhere in the world (Griffin et al., 2018). We have reported findings of Ti-bearing corundum in the kimberlite and lamproite rocks of the Ukrainian Shield and diamond-bearing sedimentary rocks (Yatsenko, 2016; Yatsenko et al., 2020).

A characteristic feature of this corundum variety is the presence of oxygen-free phases, including native iron, osbornite (TiN), khamrabaevite TiC, and intermetallic alloys of the Si-Fe, Si-Ti-Fe, Si-Al, Al-Zr-Ti-Si and Si-Cr-Fe systems. The mineral contains small pockets enclosing exotic oxides such as tistarite (Al_2O_3), hibonite $(Ca,Ce)(Al,Ti,Mg)_{12}O_{19}$, carmeltazite ($ZrAl_2Ti_4O_{11}$) as well as undefined phases of variable composition, where Al_2O_3, ZrO_2, and TiO_2 are the main components (Griffin et al., 2018; Yatsenko et al., 2020). Titanium is included in the corundum in a trivalent form (Oliveira et al., 2021), indicating that the mineral was formed under extremely reducing conditions, oxygen fugacity value estimated at less than seven logarithmic units below the iron-wustite buffer (IW-7). The presence of tistarite inclusions and highly reduced oxygen-free phases also support this inference (Griffin et al., 2018). In all known cases, corundum occurs together with HRMMA particles including spherules (TMIS and MW-I varieties), native metals, intermetallic alloys, moissanite (SiC), qusongite (WS), and diamond. Thus, Ti-bearing corundum can be considered a typical component of the HRMMA which occurs in kimberlites and other varieties of mantle rocks. Griffin et al. (2018) showed that Ti-bearing corundum is in essence a micrograined aggregate formed by skeletal crystals. From this observation, the authors concluded that the particles of the corundum aggregate studied formed as a result of the rapid cooling of extremely oversaturated Al_2O_3 melt during the explosive process. In fact, the mechanism of formation of Ti-bearing corundum is very similar to the mechanism of silicate spherule formation, as described in the next section.

Findings of corundum spherules in kimberlite breccias of the Eastern Azov region also corroborate this proposed scenario (Tatarintsev et al., 1987).

PHYSICAL CONDITIONS OF SPHERULE FORMATION

A possible mechanism for the formation of spherules associated with kimberlite rocks is as the result of the spraying of a silicate-metal melt in a gas-liquid space. The spherical shape of spherules here would be due to the action of surface tension forces on melt particles in free fluidic space to optimize the surface area to volume ratio (Wilson and Head, 2007).

Significantly, close to the melting point, silicate melts are very viscous. Viscosity decreases gradually with increasing temperature. The crucial factor for the formation of very small droplets of melt (i.e., spherules) is the temperature of melt overheating relative to the melting point, which is different for glasses of various compositions. For example, ordinary industrial glass has a melting point of ~600°C, though in order for it to become liquid enough to release gas bubbles during production it is heated to 1500°C. The relatively low temperature of the magma makes it impossible for spherules to form either during normal volcanic processes or during explosive kimberlite volcanism. Therefore, spherules with a composition corresponding to that of kimberlite magma have never been observed.

RELATIONSHIP OF KIMBERLITE AND SPHERULE FORMATION PROCESSES

A comparison of the required conditions for the formation of kimberlites and spherules, as well as their geochemical characteristics, shows their different nature. The condition of kimberlite magma generation and the conditions for the formation of the parent spherule melt are very hard to reconcile for several reasons.

First, their formation temperatures are very different. The inferred melting temperatures of CS spherule glass are in the range of 2000–2100°C (Fig. 6). A similar result was obtained by Chaikovsky and Korotchenkova (2012). Vaganov et al. (1985) estimated the melting point of TMIS glass to be ~1850°C. As this is an estimation of the lower temperature limits, the real temperature required to reach the low melt viscosity for the formation of spherules should be much higher, as noted above. The temperature of the deep kimberlite source is estimated at 1200–1400°C (Sparks et al., 2006) to 1500°C according to Mitchell (1987).

Second, the primary kimberlite melt is dominantly composed of SiO_2, MgO, FeO and CaO (Sparks et al., 2006). This melt composition is difficult to reconcile with the SiO_2-TiO_2-FeO-MnO melt of TMIS spherules or the SiO_2-CaO melt of CS spherules. Importantly, there are no known examples of substances that could represent a transitional variety between kimberlitic melts and spherule melts in terms of their composition. Even greater differences are demonstrated by the compositions of the volatile components of the kimberlites and spherules. CO_2 and H_2O are the major and necessary volatile components for the generation of kimberlitic melts (Sparks et al., 2006). The composition of the volatile components of silicate spherules from the Udachna pipe (Yakutia) and kimberlites of the Eastern Azov region consists mainly of N_2 (75–95%) with subsidiary (Bratus et al., 1987) CH_4 (4–15%), and CO_2 (0–9%). Similar compositions were obtained for spherules from the Aikhal pipe by Marshintsev (1990). A characteristic feature of the composition of volatile silicate spherules is that they are "dry", i.e., they contain no water (Vaganov et al., 1985; Bratus et al., 1987; Yatsenko et al., 2012a). We analysed the gas composition of TMIS spherules from the Mriya lamproite pipe and the Shchors kimberlite dyke (Yatsenko et al., 2013b). In both cases, the volatiles were represented by pure N_2, with no sign of water.

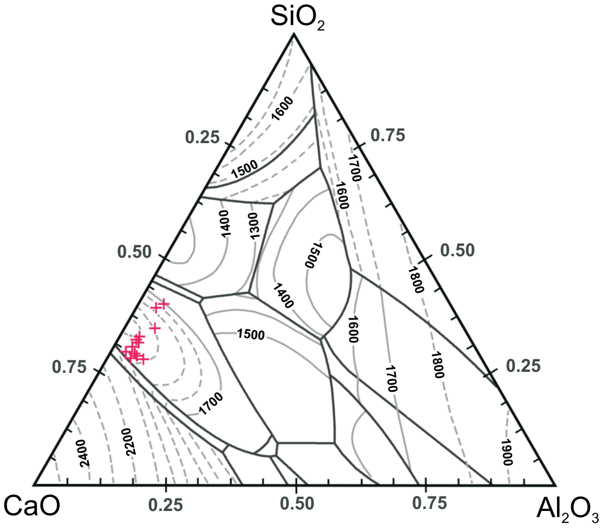

Fig. 6. Compositions (in wt.%) of CS spherules on the phase diagram for the system CaO-Al_2O_3-SiO_2 (modified after Gentile and Foster, 1963)

Third, a key observation is that spherules of different types and other components of the HRMMA never form combined aggregates (welded particles, agglutinates) neither with each other nor with kimberlite matter. At first glance, this observation seems insignificant. However, it provides evidence that the solidification of spherules from melt fragments was isolated in time and/or space from that of the kimberlite matter. This process took place in gas-melt streams, which broke through from separated volumes (magma chambers) of high-temperature (>2000°C) silicate-metal melt. Thus, spherules are xenogenic with respect to the kimberlite substance. The key question is where and how magmatic sources of specific spherule melt could be formed?

Fourth, it is known from the literature that TMIS and MW-I spherules occur not only in association with kimberlite-like rocks. Findings of spherule varieties in gold ore deposits such as Kellam (Yakutia), and the Blagodatnoye ore cluster (Far East) are known (Medvedev et al., 2006). Sandimirova recorded TMIS and MW-I spherules, Cu-Zn particles and Ti-bearing corundum in basalt-andesite volcaniclastic rocks of the Kamchatka Peninsula and the Kuril Islands. We have identified these varieties of spherules in rocks associated with the Tonkotrum (Ghana) and Muzhievo (Transcarpathia, Ukraine) gold deposits (Yatsenko et al., 2013a). Thus, spherules may be associated with different types of endogenous activity, which shows that these were formed from independent deep sources with no connection to their host rocks.

DISCUSSIONS

Many fundamental features of kimberlitic magmatism such as petrogenesis and composition of kimberlitic magma are associated with difficulties in interpretation (Sparks et al., 2006). The appearance of alien igneous entities in kimberlites, i.e., spherules, which show no affinity to kimberlites, appears enigmatic. The key question is where and how specific highly reduced melts have been generated, which represent the primary sources of melted matter for the formation of spherules.

Several suggestions for the formation of the highly reduced mantle mineral association (HRMMA), and spherules in particular, have been proposed earlier.

Marshintsev (1990) considered the formation of spherule melt in the context of the general geochemical evolution of kimberlitic melts, which tend to accumulate TiO_2, FeO, and MnO at later stages. The formation of spherules was suggested as from residual melt oversaturated with volatile components.

Chaikovsky and Korotchenkova (2012) considered that spherules could be formed as a result of differentiated condensation of evaporated matter of the host rocks. According to their hypothesis, evaporation is caused by the explosive boiling of magma supersaturated with H_2O.

Griffin et al. (1918, 2019) considered the formation of super-reduced assemblages (MW-I spherules, Ti-bearing corundum, SiC, native metals) in volcanic rocks (basalts, chromitites, kimberlites) as a result of the interaction of deep-seated magmas with abiotic mantle-derived fluids dominated by CH_4 + H_2. The redox reactions of the interaction would release CO_2 and H_2O.

These proposed scenarios for the formation of the initial melt of the spherules require the presence of melts enriched in CO_2 and H_2O, which is inconsistent with the volatile components of the spherules containing (or not containing) a very small percentage of CO_2 and no H_2O.

A fundamentally new scenario for the formation of spherules was proposed by Lukin (2006, 2013) who has studied MW-I spherules and native metal particles found in various occurrences of anthraxolite-like hydrocarbons and oil deposits and concluded that the initial formation of these hydrocarbons and associated native metals is related to processes that take place at the base of mantle plumes at the core-mantle boundary (CMB).

Yatsenko (2016, 2020) proposed that a primary silicate-metallic spherule melt formed in the CMB zone, consistent with the hypothesis of Lukin (2013). A modified concept presented here is aimed at explaining the formation of primary melts for the formation of TMIS and MW-I spherules, which are the dominant variety of kimberlite spherules.

At the base of the lower mantle lies the D'' layer, 200 km thick, directly above the CMB, and representing the boundary between the liquid iron core and the rocky silicate mantle. Garnero and McNamara (2008) state that the processes that take place in the first hundred kilometres of the lower mantle "play a critical role in the evolution of the planet". It is established that the D'' layer is chemically heterogeneous. The heterogeneity may have several causes, including reactions between the core and mantle, and partial melting in the ultra-low-velocity zone (ULVZ) located immediately above the CMB (Hirose and Lay, 2008). Strong radial and lateral temperature gradients should presumably exist in the boundary layer due to upward heat flow from the core and mantle convection (Hirose and Lay, 2008). The correlation between hotspots and the ULVZ means that the melt from the ULVZ governs the formation of plumes and their ascent to the surface (Lay et al., 1998). We propose a 2-stage scenario for the formation of the initial melt of TMIS spherules (Fe^0-TiO_2-MnO-FeO-SiO_2 melt), which commences in the ULVZ.

Stage 1 is the "reductive" stage. Garnero and McNamara (2008) stated that the ULVZ is a thermochemical zone. Thus, we can hypothesize that the crucial factor in the imbalance of chemical equilibrium and partial melting in the ULVZ may be an increase in temperature and, as a result, a decrease in oxygen fugacity (Nikolsky, 1987). If the oxygen fugacity declines then we can expect that elements having an affinity with iron (Ti, Mn, Fe, and Si) may go from an oxidized to a metallic state forming an O-Ti-Mn-Fe-Si melt (Figs. 7 and 8). Si, Ti, and Mn are stable at oxygen fugacity values slightly below the iron-wustite buffer and closer to it compared to other rock-forming elements. We have observed examples of solid Si-Ti-Fe-Mn melts that represent spherical melt inclusions in Ti-bearing corundum. Knittle and Jeanloz (1991) argued that the D" layer is a chemically active zone where an SiO_2-FeO-Fe-Si melt is formed by a reaction between $(Mg,Fe)SiO_3$ perovskite and molten iron. These conclusions are partially similar to those proposed by us.

Stage-2 is the "oxidizing" stage. If the ULVZ is interpreted as an area where mantle plumes originate (Lay et al., 1998) then uplift of the O-Ti-Mn-Fe-Si melt to shallower levels can be expected. The likelihood of such a scenario has been demonstrated by Petford et al. (2007). Vertical migration of the O-Ti-Mn-Fe-Si melt will lead to its cooling, and oxidation with transformation into a Fe^0-TiO_2-MnO-FeO-SiO_2 melt, which corresponds to the composition of the initial melt of TMIS and MW-I spherules (Fig. 8). Oxidation reactions have a pronounced exothermic effect, which can maintain the necessary high temperature of the melt during its rise to shallower low-temperature levels.

The proposed model for the formation of the initial melt of calcium-rich silicate spherules is based on an existing understanding of the mineral composition of the lower mantle. To date, bridgmanite – $(Mg,Fe)SiO_3$, ferropericlase – (Mg,Fe)O, and calcium-silicate perovskite – $CaSiO_3$ are recognized to be the main components of the lower mantle (Kaminsky, 2017, 2020). The recent discovery of calcium-silicate perovskite (named davemaoite) enclosed in diamond crystals confirms that the lower mantle is heterogeneous and that some areas of the lower mantle are enriched in this mineral (Tschauner et al., 2021). Calcium-silicate spherules from the Pivdenna pipe consist of FeO, CaO, and SiO_2, as well as native Fe and Si forming the core of the spherules. The simplest explanation for the formation of a high-calcium silicate melt with iron admixture (Fe^0-Si^0-FeO-CaO-SiO_2) may be that it is the result of the interaction of molten iron (Fe^0) and lower mantle davemaoite ($CaSiO_3$).

We acknowledge that the proposed theoretical models represent only some possible scenarios for the formation of spherule melts in the CMB region. The question of how these melts migrated at least up to the level of kimberlite melt generation remains unclear. This could be a gradual process via rise of the mantle plume or an impulsive process via an explosive breakthrough of the melt-gas mixture. Combinations of both processes are also possible. In any case, the finds of super-deep varieties of diamonds undoubtedly show the existence of pathways for the transport of matter from the lowest mantle to the near-surface environment. These deep diamond varieties contain inclusions of minerals forming the lower mantle (ferropericlase, magnesiowustite, bridgmanite, etc.), and inclusions composed of native oxygen-free phases including metals, metal alloys, carbides, and nitrides, which are thought to be the matter of the D" layer (Kaminsky, 2017, 2020).

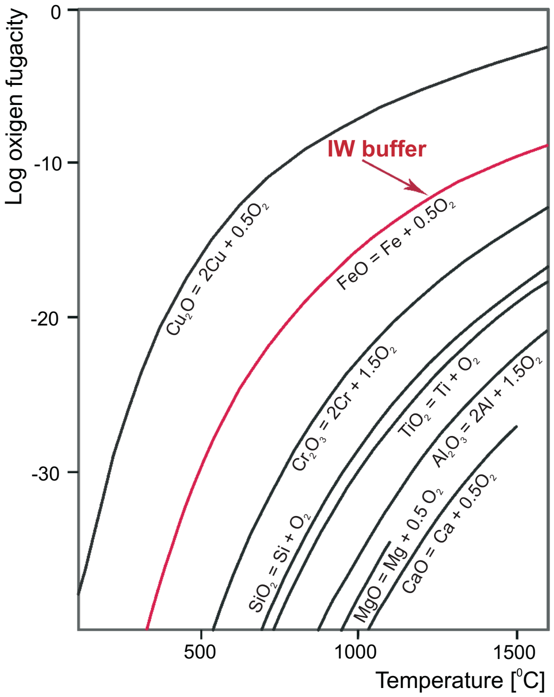

Fig. 7. Calculated element-oxide equilibrium curves at P = 1 bar (modified after Nikolsky, 1987)

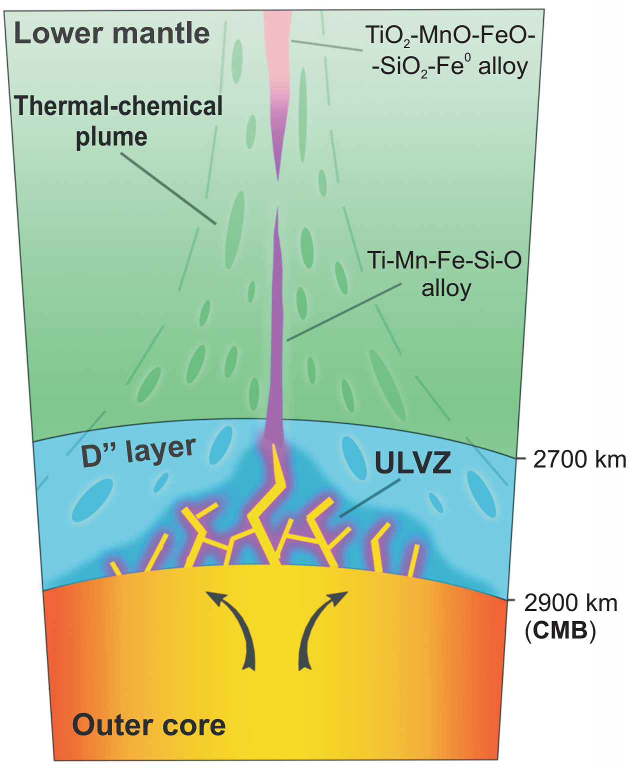

Fig. 8. Schematic cartoon showing the thermo-chemical dynamics of formation of TMIS spherule parent melt

The fact that the composition of the volatile components of the spherules is predominantly represented by N_2 is an important observation in terms of inferring the super-deep nature of the spherules (Vaganov et al., 1985; Bratus et al., 1987; Yatsenko et al., 2012b, 2013b). The bulk silicate Earth is extremely depleted in nitrogen compared to the carbonaceous chondrites that were the "building blocks" of Earth-like planets. This phenomenon is widely known as the "missing nitrogen" problem (Kaminsky and Wirth, 2017). The nitrogen balance in different geospheres remains a controversial issue; however, most researchers suggest that the bulk of nitrogen was sequestered by the Earth's metal core (Speelmanns et al., 2018; Grewal et al., 2019, 2021; Kaminsky, 2020). Kaminsky and Wirth (2017) demonstrated this possibility empirically, based on the study of nitrogen-bearing inclusions in diamonds derived from the lowermost mantle. These inclusions consist of iron nitrides (Fe_3N, Fe_2N), carbonitrides (from $M_5(C,N)_3$ to $M_{23}(C,N)_6$), nitrogen hydrides (NH_3), free nitrogen (N_2). Kaminsky (2020) concluded that iron, together with light elements (C, N), infiltrates from the outer core into D''. Kaminsky's observations and conclusions are consistent with our concept of the super-deep nature of the HRMMA, where nitrogen is a common component. Osbornite (TiN) is a common phase of Ti-bearing corundum, N_2 fills the gas bubbles of the spherules. Probably, breakthrough of nitrogen streams with melt particles was responsible for the formation and transport of spherules. Moreover, we infer that the migration of free nitrogen from the core through the base of the mantle can explain the formation of native metals (Cu, Zn, Pb, Cd, Al, Au), which are typically found in kimberlites in association with spherules (Yatsenko, 2016; Yatsenko et al., 2020). According to Le Chatelier's law, under ultrahigh-pressure conditions, nitrogen should form compounds (nitrides) with these metals. Importantly, the known nitrides of these metals are unstable ionic-covalent compounds that tend to decompose explosively: $Cu(N_3)_2$, $Zn(N_3)_2$, $Pb(N_3)_2$, Cd_3N_2, $Cd(N_3)_2$, Au_3N_2, Ag_3N, AgN_3, $Al(N_3)_3$ (Antonova et al., 1976). Thus, we infer that the gas-metal fluid migrating through the mantle can transport nitrides. The decomposition of nitrides provides an energetic contribution to the development of kimberlite magmatism. The energetic aspect of the large-scale melting of mantle rocks remains an unresolved question (Gilat and Vol, 2012). Many researchers argue that intratelluric fluid flows are determinants of energy and mass transfer from the core to the mantle and thus drive magmatic and tectonic processes (Zhatnuev, 2016). Carbon and hydrogen (Letnikov and Dorogokupets, 2001) or hydrogen and helium (Gilat and Vol, 2012) are considered to be the main energy-carrying elements. We believe that the role of nitrogen in deep fluid systems has remained underestimated; nevertheless, its ability to form unstable nitrides with some elements at ultrahigh pressures should be taken into account when reconstructing the energy balance of endogenous processes.

We believe that spherules can be successfully used as an indicator for diagnosing the admixture of pyroclastic or epiclastic (redeposited) matter of deep origin in sedimentary rocks (Morgan et al., 2004; Yatsenko et al., 2013a) and for diagnosing the nature of ring explosive structures with a controversial origin (impact or magmatic). Vaganov et al. (1985) argued that spherules from explosive endogenous structures are identical to spherules from extraterrestrial impact structures. We propose to put the question differently, i.e., the presence in the rocks of some explosive "impact" structures of spherules of indisputably endogenous origin suggests the deep nature of these explosive structures.

FINAL REMARKS AND CONCLUSIONS

Geochemical studies of spherules discovered in the kimberlite of Pivdenna pipe showed that the spherule assemblage can be divided into three distinctive varieties, including TMIS, Ca-rich silicate, and MW-I spherules. We have subdivided the Ca-rich silicate spherule into two subtypes, namely CS and CIS varieties. Native metal particles represented by native Cu and Zn have also been recognized in the samples studied. A comparative analysis shows that spherules from the Pivdenna pipe are very similar to those from the kimberlites and lamproites of the Ukraine Shield, Ural-Timan, Arkhangelsk, Yakutia, and Angola-Congo diamondiferous provinces. The formation of spherules is considered to be formed in gas-melt streams, with the instant adiabatic cooling and solidification of dispersed melt droplets. We suggest that the formation processes of the parent metal-silicate spherule melt are not related to the processes of kimberlite melt generation. According to the proposed model, the original spherule melts are formed in the CMB zone as a result of chemical interaction between molten iron and solid oxides of the lowermost mantle. Thermochemically active ULVZ zones in the D” layer may be considered the most appropriate for such processes.

We infer that nitrogen migrating from the core is responsible for the formation of native metals (Cu, Zn, Pb, and Sn), which are commonly found in kimberlites. Under ultrahigh-pressure conditions, nitrogen absorbed these metals, forming unstable nitrides. At shallower levels at low pressures, the nitrides decomposed explosively, releasing free nitrogen and native metals.

Findings of spherules and native metals in the Pivdenna pipe once again show that highly reduced particles including the spherules themselves, as well as native metals and oxygen-free minerals, are a common component of kimberlite-lamproite rocks. Spherules can thus be used in the exploration of diamondiferous rocks in the same way that kimberlite indicator minerals are used for this purpose.

The inferred features of the formation of the studied spherules allow us to consider their formation as a special class of magmatic activity of the Earth. Characteristic features of these processes are the high temperature of the melt, the highly reduced conditions, the strictly defined composition of the melt, and the super-deep nature of igneous sources.

Acknowledgements. Dr K. Nejbert and an anonymous reviewer are kindly acknowledged for their qualified comments.

REFRENCES

Antonova, M.M., Brakhnova I.T., Borisova, A.I., Dvorina, L.A., Drozdova, S.V., Kosolapova, T.Ya., Kulik, O.P., Lynchak, K.A., Obolonchik, V.A., Panasyuk, A.D., Popova, O.I., Samsonov, G.V., Semenov-Kobzar, A.A., Serebryakova, T.I., Sinelnikova, V.S., Chernogorenko, V.B., Yanaki, A.A., 1976. Element Properties. Part 2. Chemical Properties (in Russian). Metalurgiya, Moscow.

Badjukov, D.D., Jouko, R., 2003. Micrometeorites from the northern ice cap of the Novaya Zemlya arhipelago, Russia: The first occurrence. Meteoritics and Planetary Science, **38**: 329–340. https://doi.org/10.1111/j.1945-5100.2003.tb00269.x

Berczi, Sz., Lukacs, B., Torok, K., 1999. Snouted Spherules: in the Carpathian Basin and on Antarctica. Hungarian Academy of Sciences, Central Research Institute for Physics, Budapest.

Bratus, M.D., Tatarintsev, V.I., Sakhno, B.E., 1987. The composition of fluid inclusions the hardened particles from explosive ring structures and kimberlite pipes (in Russian). Geokhimiya, **11**: 1563–1568.

Brown, G.M., Emeleus, C.H., Grenville, H.J., Phillips, R.P., 1970. Petrographic, mineralogic, and x-ray fluorescence analysis of lunar igneous-type rocks and spherules. Science, **167** 599–601. https://doi.org/10.1126/science.167.3918.599

Chaikovsky, I.I., Korotchenkova, O.V., 2012. Explosive mineral phases from Western Urals diamondiferous visherites (in Russian with English summary). Lithosphera, (2): 125–140.

Culler, T.S., Muller, R.A., Renne, P., 1997. Use of lunar spherules to determine the terrestrial cratering rate over the last 3 Ga. Meteoritics and Planetary Science, **32**: A32.

Dawson, J.B., 1980. Kimberlites and their Xenoliths. Springer, Berlin-Heidelberg-New York.

El Coresy, A., 1968. Electron microprobe analysis and ore microscopic study of magnetic spherules and grains collected from the Greenland ice. Contributions to Mineralogy and Petrology, **17**: 331–346.

Firestone, R.B., West, A., Kennett, J.P., Becker, L., Bunch, T.E., Revay, Z.S., Schultz, P.H., Belgya, T., Kennett, D.J., Erlandson, J.M., Dickenson, O.J., Goodyear, A.C., Harris, R.S., Howard, G.A., Kloosterman, J.B., Lechler, P., Mayewski, P.A., Montgomery, J., Poreda, R., Darrahp, T., Que Hee, S.S., Smith, A.R., Stich, A., Topping, W., Wittke, J.H., Wolbach, W.S., 2007. Evidence for an extraterrestrial impact 12,900 years ago that contributed megafaunal extinctions and the Younger Drias cooling. PNAS, **104**: 16016–16021. https://doi.org/10.1073/pnas.0706977104

Fredriksson, K., Dube, A., Milton, D.J., Balasundaram, M.S., 1973. Lonar lake, India: an impact crater in basalt. Science, **180**: 862–864. https://doi.org/10.1126/science.180.4088.862

Garnero, E., McNamara, A.K., 2008. Structure and dynamics of Earth’s lower mantle. Science, **320**: 626–628. https://doi.org/10.1126/science.1148028

Geiko, Yu.V., Gurskyi, D.S., Lykov, L.I., Metalidi, V.S., Pavlyuk, V.N., Prykhodko, V.L., Tsymbal, S.N., Shumkiv, L.M., 2006. Perspectives of basement diamond productivity of Ukraine (in Russian). Tsentr Yevropy, Kyiv.

Gentile, A.L., Foster, W.R., 1963. Calcium hexaluminate and its stability relations in the system CaO-Al$_2$O$_3$-SiO$_2$. Journal of the American Ceramic Society, **46**: 74–76.

Gilat, A.L., Vol, A., 2012. Degassing of primordial hydrogen and helium as the major energy source for internal terrestrial processes. Geoscience Frontiers, **3**: 911–921. https://doi.org/10.1016/j.gsf.2012.03.009

Glass, B.P., Burns, C.A., Crosbie, J.R., Dubois, D.L., 1985. Late Eocene North American microtektites and clinopyroxene-bearing spherules. Journal of Geophysical Research, **90**: 175–196.

Grachev, A.F., Korchagin, O.A., Tselmovich, V.A., Kollmann, H.A., 2008. Cosmic dust and micrometeorites in the transitional clay layer at the Cretaceous–Paleogene boundary in the Gams section (Eastern Alps): morphology and chemical composition. Physics of the Solid Earth, **44**: 555–569. https://doi.org/10.1134/S1069351308070069

Graup, G., 1981. Terrestrial chondrules, glass spherules and accretionary lapilli from the suevite, Ries Crater, Germany. Earth and Planetary Science Letters, **55**: 407–418. https://doi.org/10.1016/0012-821X(81)90168-0

Grewal, D.S., Dasgupta, R., Holmes, A.K., Costin, G., Li, Yu., Tsuno, K., 2019. The fate of nitrogen during core-mantle separation on Earth. Geochimica et Cosmochimica Acta, **251** 87–115. https://doi.org/10.1016/j.gca.2019.02.009

Grewal, D.S., Dasgupta, R., Hough, T., Farnell, A., 2021. Rates of protoplanetary accretion and differentiation set nitrogen budget of rocky planets. Nature Geoscience, **14**: 369–376. https://doi.org/10.1038/s41561-021-00733-0

Griffin, W.L., Huang, J.-X., Thomassot, E., Gain, S.E.M., Toledo, V., O'Reilly, S.Y., 2018. Super-reducing conditions in ancient and modern volcanic systems: sources and behaviour of carbon-rich fluids in the lithospheric mantle. Mineralogy and Petrology, **112**: 101–114. https://doi.org/10.1007/s00710-018-0575-x

Griffin, V.L., Gain, S.E.M., Huang, J.-X., Saunders, M., Toledo, V., O'Reilly, S.Y., 2019. A terrestrial magmatic hibonite-grossite-vanadium assemblage: desilication and extreme reduction in a volcanic plumbing system, Mount Carmel, Israel. American Mineralogist, **104**: 207–219. https://doi.org/10.2138/am-2019-6733

Gursky, D.S., 2008. The Conception of the State Industrial Raw-Materials Politic of the Use of the Strategic Significant for the Country Economic Materials and Rocks (in Ukrainian). ZUKTs, Lviv.

Hefferan, K., O'Brien, J., 2010. Earth Materials. Wiley-Blackwell, Chichester, West Sussex, UK.

Hirose, K., Lay, T., 2008. Discovery of post-perovskite and new views on the core-mantle Boundary Region. Elements, **4**: 181–186. https://doi.org/10.2113/GSELEMENTS.4.3.181

Hodge, P.W., 1973. Lunar and terrestrial impact crater spherules. The Moon, **7**: 483–486. https://doi.org/10.1007/BF00564648

Kaminsky, F., Wirth, R., 2017. Nitrides and carbonitrides from the lowermost mantle and their importance in the search for Earth's "lost" nitrogen. Amĺrican Mineralogist, **102**: 1667–1676. https://doi.org/10.1007/978-3-319-55684-0

Kaminsky, F.V., 2017. The Earth's Lower Mantle. Composition and Structure. Springer Geology, Cham. https://doi.org/10.1007/978-3-319-55684-0_1

Kaminsky, F.V., 2020. Basic problems concerning the composition of the Earth's lower mantle. Lithos, **364–365**: 105515. https://doi.org/10.1016/j.lithos.2020.105515

Knittle, E., Jeanloz, R., 1991. Earth's core-mantle boundary: Results of experiments at high pressures and temperatures. Science, **251**: 1438–1443. https://doi.org/10.1126/science.251.5000.1438

Lay, T., Williams, Q., Garnero, E.J., 1998. The core-mantle boundary layer and deep Earth dynamics. Nature, **392**: 461–468. https://doi.org/10.1038/33083

Letnikov, F.A., Dorogokupets, P.I., 2001. The role of superdeep fluid systems of the Earth's core in endogenous geological processes (in Russian with English summary). Doklady AN, **378**: 535–537.

Lukin, A.E., 2006. Native metals and carbides – marks of compositions of deep geospheres (in Russian with English summary). Geologicheskiy Zhurnal, (4): 17–46.

Lukin, A.E., 2013. Mineral spherules – particular fluidic mode of ore and oil genesis (in Russian with English summary). Geofizicheskiy Zhurnal, **35**: 10–53.

Makeyev, V.A., Kriulina, G.Yu., 2012. Metal films on the surfaces and within diamond crystals from Arkhangelskaya and Yakutian diamond provinces. Geology of Ore Deposits, **54**: 663–673. https://doi.org/10.1134/S1075701512080107

Marshintsev, V.K., 1990. The nature of spheroid formations in kimberlites (in Russian). In: Traces of Cosmic Impact on the Earth (ed. A.N. Dmitriev): 45–57. Nauka, Novosibirsk.

Medvedev, Ye.I., Molchanov, V.P., Khomich, V.G., 2006. Palladium-bearing gold, magnetite and shorlomite microspherules from placers of the Blagodatnensk cluster (Primorie), and their possible sources. Russian Journal of Pacific Geology, **25**: 92–96.

Mitchell, R.H., 1987. Kimberlites, Mineralogy, Geochemistry, and Petrology. Plenum Press, New York.

Morgan, J.P., Reston, T.J., Ranero, C.R., 2004. Contemporaneous mass extinctions, continental flood basalts, and 'impact signals': are mantle plume-induced lithospheric Earth and gas explosions the causal link? Earth and Planetary Science Letters, **217**: 263–284. https://doi.org/10.1016/S0012-821X(03)00602-2

Nikolsky, N.S., 1987. Fluid Regime of Endogenous Ore Formation (in Russian). Nauka, Moskow.

Novgorodova, M.I., Gamyanin, G.N., Zhdanov, Yu.A., Agakhanov, T.V., Dikaya. T.V., 2003. Aluminosilicate glass microspherules in gold ores (in Russian). Geokhimiya, (1): 89–93.

O'Keefe, J.A., 1986. Eocene microtektites and clinopyroxene-bearing spherule. Lunar and Planetary Science, **17**: 630–631.

Oliveira, B., Griffin, W.L., Gain, S.E.M., Saunders, M., Shaw, J., Toledo, V., Afonso, J.C., O'Reilly, S.Y., 2021. Ti^{3+} in corundum traces crystal growth in a highly reduced magma. Scientific Reports, **2439**: 1–12. https://doi.org/10.1038/s41598-020-79739-4

Peskov, E.G., 2000. Geologic Evidence of the Earth's Cold Degasing (in Russian with English summary). NEISRI FEB RAS, Magadan.

Petford, N., Rushmer, T., Yuen, D.A., 2007. Deformation-induced mechanical instabilities at the core-mantle boundary. In: Post-Perovskite: the Last Mantle Phase Transition (eds. K. Hirose, J. Brodholt, T. Lay and D. Yuen): 271–287. Geophysical Monograph Series, **174**. https://doi.org/10.1029/174GM18

Robin, E., Froget, L., Jehanno, C., Rocchia, R., 1993. Evidence for a K/T impact event in the Pacific Ocean. Nature, **363** 615–617.https://doi.org/10.1038/363615a0

Rychagov, S.N., Glavatskikh, S.F., Sandimirova, Ye.I., 1997. Ore and silicate magnetic spherules as indicators of the structure and fluid regime of the modern Baransky hydrothermal system, Iturup Island (in Russian). Doklady AN, **356**: 677–681.

Sandimirova, Ye.I., Glavatskikh, S.F., Rychagov, S.N., 2003. Magnetic spherules from volcanogenic rocks of the Kuril Islands and South Kamchatka (in Russian). Vestnik KRAUNTS. Nauki o Ziemle, (1): 135–140.

Sheremet, E.M., Kozyr, N.A., Strekozov, S.N., Chashka, A.I., Bondarenko, V.A., Fedorishin, Yu.I., Pigulevsky, P.I., 2014. Explorations for Diamonds in the Azov Block of Ukrainian Shield (in Russian). Noulidzh, Donetsk.

Sparks, R.S.J., Baker, L., Brown, R.J., Field, M., Schumaher, J., Stripp, J., Walters, A., 2006. Dynamical constrains on kimberlite volcanism. Journal of Volcanology and Geothermal Research, **155**: 18–48. https://doi.org/10.1016/j.jvolgeores.2006.02.010

Speelmanns, I.M., Max, W., Schmidt, M.W., Liebske, C., 2018. Nitrogen solubility in core materials. Geophysical Research Letters, **45**: 7434–7443. https://doi.org/10.1029/2018GL079130

Tatarintsev, V.I., Tsymbal, S.N., Garanin, V.K., Kudryavtseva, G.P., Marshintsev, V.K., 1983. Hardened particles from kimberlites of Yakutia (in Russian). Doklady AN SSSR, **270**: 1199–1203.

Tatarintsev, V.I., Sandomirskaya, S.M., Tsymbal, S.N., 1987. The first discovery of titanium nitride (osbornite) in the rocks of the Earth (in Russian). Doklady AN SSSR, **296**: 1458–1461.

Taylor, S., Lever, J.H., Harvey, R.P., 2000. Number, types and compositions of an unbiased collection of cosmic spherules. Meteoritics and Planetary Science, **35**: 651–666. https://doi.org/10.1111/j.1945-5100.2000.tb01450.x

Tischenko, A.I., 2004. Gold and other native metals in kimberlites of the Eastern Azov region (in Ukrainian). In: Prospects for Diamond Potential on Ukraine Territories (ed. D.S. Gursky): 106–111. UkrDGRI, Kyiv.

Tschauner, O., Huang, S., Yang, S., Humayun, M., Liu, W., Corder, S.N.G., Bechtel, H.,A., Tischler, J., Rossman, G.R., 2021. Discovery of davemaoite, $CaSiO_3$-perovskite, as a mineral from the lower mantle. Science, **374**: 891–894. https://doi.org/10.1126/science.abl8568

Tsymbal, S.N., Kvasnitsa, V.N., Tsymbal, Yu.S., Melnichuk, E.V., 1999. Diamond from impactites of Belilovskaya (Western) astrobleme (in Russian). Mineralogycheskiy Jurnal, **21**: 45–52.

Uzonyi, I., Kiss, A.Z., Solt, P., Dosztaly, L., Kakay Szabo, O., Detre, Cs.H., 1998. Analysis of glassy spherules extracted from Carpathian Mesozoic limestone by IPIXE method. Nuclear Instruments and Methods in Physics Research, **139**: 192–195.

Vaganov, V.I., Ivankin, P.F., Kropotkin, P.N., Trukhalev, A.I., Semenenko, N.P., Tsymbal, C.N., Tatarintsev, V.I., Glukhovsky, M.Z., Bulgakov, E.A., 1985. Explosive Ring Structures of Shields and Platforms (in Russian). Nedra, Moskow.

Wilson, L., Head, J.W., 2007. An integrated model of kimberlite ascent and eruption. Nature, **447**: 53–57.
https://doi.org/10.1038/nature05692

Yatsenko, I.G., 2016. Silicate-metallic spherules in explosive and sedimentary formations of Ukraine. Genetic and prospecting aspects (in Ukrainian with English summary). Ph.D. Thesis, Ivan Franko University of Lviv.

Yatsenko, G.M., Gursky, D.S., Slivko, E.M., Geyko, Yu.V., Prihodko, V.L., Rosihina, A.I., Drosdetsky, V.V., Yatsenko, V.G., 2002. Diamondiferous formations and structures on the southwest side of East-European platform (in Russian). UkrDGRI, Kyiv.

Yatsenko, I., Yatsenko, G., Bekesha, S., Bilyk, N., Varychev, A., Druchok, L., 2012a. Endogenous Ti-Mn-Fe silicate spherules from explosive structures and volcanic-sedimentary formations of Ukraine (in Ukrainian with English summary). Mineralogichnyi zbirnyk, **62**: 83–101.

Yatsenko, I., Yatsenko, G., Naumko, I., S.N., Bekesha, S., Bilyk, N., Shvayevskyi, O., 2012b. Volatile components in endogenous spherules and the problem of fluidised-explosive ore genesis (in Ukrainian with English summary). Mineralogichnyi Zbirnyk, **62**: 189–199.

Yatsenko, I.G., Bilyk, N.T., Kuderavets, R.S., Tymoshuk, V.R., Shvayevsky, A.V., 2013a. Explosive mantle-derived particles in sedimentary formations of the Carpathian region, connection with the problem of fuels and ore deposits formation (in Russian with English summary). Geodinamica, **15**: 72–74.
https://doi.org/10.23939/jgd2013.02.072

Yatsenko, I.G., Yatsenko, G.M., Naumko, I.M., Bekesha, S.N. Sahno, B.E., 2013b. Composition of volatile components in endogenous spherules. Abstracts of XXX international conference “Alcaline magmatism of the Earth”. GEOHI RAN, Moscow: 62–63.
http://alkaline.web.ru/2013/abstracts/Yatsenko.htm

Yatsenko, I.G., Skublov, S.G., Levashova, E.V., Galankina, O.L., Bekesha S.N., 2020. Composition of spherules and lower mantle minerals, isotopic and geochemical characteristics of zircon from volcaniclastic facies of the Mriya lamproite pipe. Journal of Mining Institute, **242**: 150–159.
https://doi.org/10.31897/PMI.2020.2.150

Zhatnuev, N.S., 2016. Transmantle (intratelluric) fluid flows. a new model for plumes and plume magmatism (in Russian with English summary). Geologiya i geofisika, **57**: 1445–1454.
http://dx.doi.org/10.15372/GiG20160802

Zinchenko, V., Dech, V., Shafranovsky, G., 2012. Kimberlites and Diamonds of Katoka Pipe: Petrogenesis, Ore Genesis and Modeling the Distribution of Diamonds. Palmarium Academic Publishing, Saarbrücken.